

# Cyclopentadienyl( $\eta^4$ -*trans*-diene)nitrosylmolybdenum Complexes and Their Reactivities toward Acetylenes and Protonic Acids<sup>1,2</sup>

Nancy J. Christensen and Peter Legzdins\*

Department of Chemistry, The University of British Columbia, Vancouver, British Columbia, Canada V6T 1Z1

Frederick W. B. Einstein\* and Richard H. Jones

Department of Chemistry, Simon Fraser University, Burnaby, British Columbia, Canada V5A 1S6

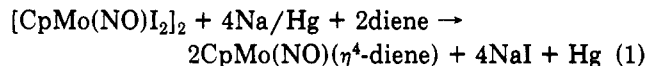
Received March 12, 1991

Reduction of  $[\text{Cp}^*\text{Mo}(\text{NO})\text{I}_2]_2$  [ $\text{Cp}^* = \eta^5\text{-C}_5\text{Me}_5$ ] by sodium amalgam in THF at  $-30^\circ\text{C}$  in the presence of an isomeric mixture of (*E*)- and (*Z*)-1,3-pentadiene affords two isolable isomers of  $\text{Cp}^*\text{Mo}(\text{NO})(\eta^4\text{-trans-1,3-pentadiene})$ , one yellow (**1A**) and one red (**1B**). The most significant feature of the solid-state molecular structure of **1A** is the fact that the transoidal (*E*)-1,3-pentadiene ligand is coordinated to the molybdenum with its methyl substituent pointing away from the cyclopentadienyl ring. The spectroscopic properties of **1B** are consistent with it possessing a similar orientation of its (*Z*)-1,3-diene methyl substituent. This observation establishes that even though the  $\text{Cp}^*\text{Mo}(\text{NO})$  fragment in **1A** and **1B** exerts the electronic influence to bind the diene ligands in a twisted, transoidal fashion, steric interactions determine which face of the diene ligand can best accommodate this electronic requirement. Cyclic voltammetry studies have been carried out on two representative diene-containing compounds, namely  $\text{CpMo}(\text{NO})(\eta^4\text{-trans-2,5-dimethyl-2,4-hexadiene})$  and  $\text{CpMo}(\text{NO})(\eta^4\text{-cis-2,3-dimethylbutadiene})$  ( $\text{Cp} = \eta^5\text{-C}_5\text{H}_5$ ), in order to establish the redox properties of these types of complexes. The cyclic voltammograms indicate that both diene complexes are reasonably stable with respect to addition of electrons, since no reduction behavior is observed to the limit of the  $\text{CH}_2\text{Cl}_2$  solvent (ca.  $-2\text{ V}$ ). On the other hand, each of the complexes is quite readily oxidized and each exhibits three irreversible oxidations before the solvent limit of ca.  $+2\text{ V}$ . These redox properties are in accord with the results of Fenske-Hall molecular orbital calculations previously performed on the  $\text{CpMo}(\text{NO})(\eta^4\text{-butadiene})$  model systems. Consistently,  $\text{CpMo}(\text{NO})(\eta^4\text{-trans-2,5-dimethyl-2,4-hexadiene})$  does not undergo concomitant reduction when treated with acetylenes but rather effects a coupling between the diene ligand and the alkyne to produce a  $\eta^4(\eta^3, \eta^1)$  ligand in which the  $\eta^3$ -allyl portion of the ligand is oriented endo with respect to the cyclopentadienyl ring. Thus, when the alkyne employed is 1-phenylpropyne, the resulting complex is  $\text{CpMo}(\text{NO})[\eta^4\text{-C}(\text{Me})_2\text{CHCHC}(\text{Me})_2\text{C}(\text{Me})\text{C}(\text{Ph})]$  (**2**), whose molecular structure has been established by specialized NMR spectroscopic techniques and by single-crystal X-ray crystallography. The reaction between  $\text{CpMo}(\text{NO})(\eta^4\text{-trans-2,5-dimethyl-2,4-hexadiene})$  and 1,7-octadiyne affords two major isomers of a similar organometallic product. Finally, the isolable products of the reactions between  $\text{CpMo}(\text{NO})(\eta^4\text{-trans-diene})$  and  $\text{HX}$  (diene = 2,5-dimethyl-2,4-hexadiene,  $\text{HX} = \text{HI}$ ,  $\text{HO}_3\text{SC}_6\text{H}_4\text{CH}_3$ ,  $\text{HO}_2\text{CCF}_3$ ; diene = butadiene,  $\text{HX} = \text{HI}$ ) are the  $\eta^3$ -allyl complexes  $\text{CpMo}(\text{NO})(\eta^3\text{-allyl})(\text{X})$  (**4-7**), in which the allyl linkage is asymmetrically ( $\sigma$ ,  $\pi$ ) bound to the metal. In solutions these latter complexes exist as mixtures of isomers. Crystals of  $\text{Cp}^*\text{Mo}(\text{NO})(\eta^4\text{-trans-(E)-1,3-pentadiene})$  (**1A**) are monoclinic,  $P2_1/c$ , with  $a = 7.312$  (1) Å,  $b = 14.535$  (3) Å,  $c = 14.602$  (5) Å,  $\beta = 103.38$  (2)°, and  $Z = 4$ ; the structure was solved by conventional heavy-atom methods and was refined by full-matrix least-squares procedures to  $R = 0.046$  and  $R_w = 0.057$  for 2229 absorption-corrected reflections with  $I > 3\sigma(I)$ . Crystals of  $\text{CpMo}(\text{NO})[\eta^4\text{-C}(\text{Me})_2\text{CHCHC}(\text{Me})_2\text{C}(\text{Me})\text{C}(\text{Ph})]$  (**2**) are triclinic,  $P\bar{1}$ , with  $a = 7.973$  (2) Å,  $b = 9.330$  (1) Å,  $c = 14.324$  (2) Å,  $\alpha = 73.04$  (1)°,  $\beta = 89.33$  (2)°,  $\gamma = 72.96$  (2)°, and  $Z = 2$ ;  $R = 0.018$  and  $R_w = 0.024$  for 2976 reflections.

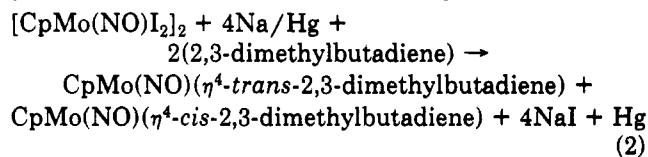
## Introduction

The first diene complex containing the  $\text{CpMo}(\text{NO})$  fragment ( $\text{Cp} = \eta^5\text{-C}_5\text{H}_5$ ) was prepared in our laboratories in 1983,<sup>3</sup> and the unique modes of coordination of the diene ligands to the metal centers in these species were delineated in two subsequent communications.<sup>4,5</sup> These organometallic complexes are generally prepared via the sodium amalgam reduction of  $[\text{CpMo}(\text{NO})\text{I}_2]_2$  in THF in the presence of the acyclic, conjugated diene, as summa-

rized in eq 1. In most cases, the organometallic products



of reactions 1 are the  $\eta^4$ -*trans*-diene complexes,  $\text{CpMo}(\text{NO})(\eta^4\text{-trans-diene})$ . Interestingly, when the diene employed is 2,3-dimethylbutadiene, two diene-containing products are isolable, as indicated in eq 2. The *cis*-diene



complex is the kinetic product and converts in solution irreversibly to its thermodynamically more stable *trans*-diene isomer. Reactions 1 and 2 have subsequently been extended to encompass an extensive series of diene ligands as well as some of their  $\text{Cp}^*$  analogues, i.e.  $\text{Cp}^*\text{Mo}(\text{NO})(\eta^4\text{-trans-diene})$  and  $\text{Cp}^*\text{Mo}(\text{NO})(\eta^4\text{-cis-2,3-dimethylbutadiene})$  ( $\text{Cp}^* = \eta^5\text{-C}_5\text{Me}_5$ ).<sup>6</sup>

(1) Organometallic Nitrosyl Chemistry. 47. For part 46, see: Legzdins, P.; Rettig, S. J.; Ross, K. J.; Veltheer, J. E. *J. Am. Chem. Soc.* 1991, 113, 4361.

(2) (a) Taken in part from: Christensen, N. J. Ph.D. Dissertation, The University of British Columbia, 1989. (b) Presented in part at the 1989 International Chemical Congress of Pacific Basin Societies (PACIFICHEM 1989), Honolulu, HI, Dec 1989; Abstract ORGN 314.

(3) Nurse, C. R. Ph.D. Dissertation, The University of British Columbia, 1983.

(4) Hunter, A. D.; Legzdins, P.; Nurse, C. R.; Einstein, F. W. B.; Willis, A. C. *J. Am. Chem. Soc.* 1985, 107, 1791.

(5) Hunter, A. D.; Legzdins, P.; Nurse, C. R.; Einstein, F. W. B.; Willis, A. C.; Bursten, B. E.; Gatter, M. G. *J. Am. Chem. Soc.* 1986, 108, 3843.

In this paper we report the results of our further investigations of the characteristic physical and chemical properties of these unusual diene-containing compounds. Specifically, we first describe the synthesis and characterization of the two isomers Cp\*Mo(NO)[ $\eta^4$ -trans-(*E* or *Z*)-1,3-pentadiene], which strikingly illustrate that steric factors play a role in determining which face of the diene ligands is linked in a transoidal fashion to the metal centers. We then present the redox properties of representative CpMo(NO)( $\eta^4$ -diene) complexes as determined by cyclic voltammetry and establish that these properties are in accord with the currently held views of the bonding extant in these organometallic species. Finally, we describe the characteristic reactivities of typical CpMo(NO)( $\eta^4$ -trans-diene) complexes toward acetylenes and protonic acids. These reactivity patterns provide additional supporting evidence concerning the distribution of the valence electrons in the organometallic reactants.

### Experimental Section

All reactions and subsequent manipulations involving organometallic reagents were performed under anaerobic and anhydrous conditions by using an atmosphere of dinitrogen. Conventional Schlenk techniques or a Vacuum Atmospheres Corporation Dri-Lab Model HE-43-2 drybox were employed for the manipulation of air- and moisture-sensitive compounds.<sup>7</sup> All reagents were purchased from commercial suppliers or were prepared according to their published procedures. Reagent purity was ascertained by elemental analysis and <sup>1</sup>H NMR spectroscopy. Florisil (60–100 mesh) was used for the preparation of chromatography columns. Solvents were dried according to conventional procedures,<sup>8</sup> distilled and deaerated with dinitrogen just prior to use.

Infrared spectra were recorded on a Nicolet 5DX FT-IR spectrometer which was internally calibrated with a He/Ne laser. Proton and carbon-13 nuclear magnetic resonance spectra were recorded on either a Varian XL-300 or Bruker WH-400 spectrometer with reference to the residual <sup>1</sup>H or <sup>13</sup>C signal of the solvent employed (usually C<sub>6</sub>D<sub>6</sub>). All <sup>1</sup>H and <sup>13</sup>C chemical shifts are reported in parts per million (ppm) downfield from Me<sub>4</sub>Si. Ms. M. Austria, Ms. L. Darge, and Dr. S. O. Chan assisted in the collection of some of the NMR spectra. Low-resolution mass spectra were recorded at 70 eV on an Atlas CH4B or a Kratos MS50 spectrometer by using the direct-insertion method by Dr. G. K. Eigendorf and the staff of the UBC Mass Spectrometry Laboratory; probe temperatures were between 100 and 150 °C. Elemental analyses were performed by Mr. P. Borda at UBC.

**NMR Experiments.** Some nonroutine NMR experiments were conducted during this study. The specific experiments are described below.

**(a) 2-Dimensional Heterocorrelation NMR Experiments (2D-HETCOR).** Varian's 2D-HETCOR pulse program was used in these experiments. The 90° <sup>13</sup>C pulse was 18  $\mu$ s, the 90° <sup>1</sup>H pulse from the decoupler was 46  $\mu$ s, the acquisition time was ca. 0.6 s, and presaturation was used. The number of incremental spectra was determined according to the concentration of the sample and spectral width used for collection of the FIDs. Zero-filling and a 2D-Fourier transformation resulted in a spectrum with a resolution of ca. 6 and ca. 100 Hz in the proton and carbon dimensions, respectively. Depending on the specific requirements of the experiments, spectra with adequate signal-to-noise ratios were obtained in 6–16 h.

**(b) Selective Insensitive Nuclei Enhancement through Polarization Transfer (SINEPT).** These experiments were

performed with Varian's pulse sequences on the XL-300 spectrometer. These spectra were collected with a 90° <sup>13</sup>C pulse of 18  $\mu$ s. The low-power proton pulse from the decoupler was 46  $\mu$ s. The decoupler was on during acquisitions (0.4 s) and off between acquisitions (2 s). The number of incremental spectra was determined according to the concentration of the individual samples, and spectra with adequate signal-to-noise ratios were obtainable in 4–12 h.

**Reduction of [Cp\*Mo(NO)I<sub>2</sub>]<sub>2</sub> in the Presence of 1,3-Pentadiene.** In a 300-mL, 3-necked round-bottom flask was mixed 25.0 g of Na/Hg (1.3 mmol of Na/g, 32.5 mmol Na) and 5–7 mL of Hg. When the mixture had liquefied, THF (100 mL) was added, and the system was cooled to ca. –30 °C by using a saturated CaCl<sub>2</sub>(aq)/dry ice bath. Then 1,3-pentadiene (piperylene, mixture of isomers, 1 mL) and [Cp\*Mo(NO)I<sub>2</sub>]<sub>2</sub><sup>3,9</sup> (5.15 g, 5.0 mmol) were added to the stirred solution. As the reaction mixture was stirred, the progress of the reaction was followed by IR spectroscopy. After approximately 1 h, the reaction was deemed to be complete when the only  $\nu_{\text{NO}}$  band evident in an IR spectrum of the reaction solution was one at 1586 cm<sup>-1</sup>. The supernatant solution was quickly cannulated away from the mercury residue into a separate flask, and its solvent was removed in vacuo to leave a brown residue. This residue was extracted with Et<sub>2</sub>O (4  $\times$  50 mL) to obtain a dark yellow solution ( $\nu_{\text{NO}}$  1597 cm<sup>-1</sup>). The combined extracts were again taken to dryness under reduced pressure, and the resultant brown residue was extracted with hexanes (4  $\times$  50 mL) to obtain a yellow solution whose IR spectrum exhibited a  $\nu_{\text{NO}}$  at 1607 cm<sup>-1</sup>. The hexanes extracts were combined and concentrated to ca. 30 mL in vacuo whereupon they were eluted through a Florisil column (3  $\times$  12 cm) with hexanes as eluant. The first band to develop and be eluted was yellow. Collection of this band followed by concentration of the eluate to ca. 10 mL afforded a yellow solution ( $\nu_{\text{NO}}$  1607 cm<sup>-1</sup>). This yellow solution was stored at –20 °C for 1 week to permit the growth of yellow crystals of Cp\*Mo(NO)( $\eta^4$ -trans-(*E*)-1,3-pentadiene) (1A) in 31% yield. A crystal suitable for a single-crystal X-ray crystallographic analysis was selected from the material obtained in this manner.

Anal. Calcd for C<sub>15</sub>H<sub>23</sub>NOMo: C, 54.68; H, 7.20; N, 4.29. Found: C, 54.74; H, 7.00; N, 4.26. IR (CH<sub>2</sub>Cl<sub>2</sub>):  $\nu_{\text{NO}}$  1568 cm<sup>-1</sup>. IR (THF):  $\nu_{\text{NO}}$  1586 cm<sup>-1</sup>. Low-resolution mass spectrum (probe temperature 120 °C): *m/z* 331 (P<sup>+</sup>, <sup>98</sup>Mo). The <sup>1</sup>H and <sup>13</sup>C NMR data for 1A are summarized in Table I.

The second band ( $\nu_{\text{NO}}$  1607 cm<sup>-1</sup>) to be eluted from the Florisil column was red. Collection and concentration of this band, followed by cooling to –20 °C for 1 week, resulted in the isolation of Cp\*Mo(NO)( $\eta^4$ -trans-(*Z*)-1,3-pentadiene) (1B) as an analytically pure, microcrystalline red solid in 11% yield.

Anal. Calcd for C<sub>15</sub>H<sub>23</sub>NOMo: C, 54.68; H, 7.20; N, 4.29. Found: C, 54.54; H, 7.00; N, 4.26. IR (CH<sub>2</sub>Cl<sub>2</sub>):  $\nu_{\text{NO}}$  1568 cm<sup>-1</sup>. IR (THF):  $\nu_{\text{NO}}$  1586 cm<sup>-1</sup>. Low-resolution mass spectrum (probe temperature 120 °C): *m/z* 331 (P<sup>+</sup>, <sup>98</sup>Mo). The <sup>1</sup>H and <sup>13</sup>C NMR data for 1B are also presented in Table I.

**Electrochemical Studies of CpMo(NO)( $\eta^4$ -trans-2,5-dimethyl-2,4-hexadiene)<sup>6</sup> and CpMo(NO)( $\eta^4$ -cis-2,3-dimethylbutadiene)<sup>6</sup> in CH<sub>2</sub>Cl<sub>2</sub>.** Electrochemical measurements were accomplished with a PAR Model 173 potentiostat equipped with a Model 176 current-to-voltage converter and a Model 178 electrometry probe, using a three-electrode cell and methods described previously.<sup>10</sup> All potentials are reported versus the aqueous saturated calomel electrode (SCE). Compensation for *iR* drop in potential measurement was not employed in this study. The [n-Bu<sub>4</sub>N]PF<sub>6</sub> support electrolyte was prepared according to the published procedure.<sup>10a</sup> The CH<sub>2</sub>Cl<sub>2</sub> was obtained from BDH Chemicals (spectral grade) and was stirred over alumina (Woelm neutral, activity 1) while simultaneously being purged with N<sub>2</sub> for 15 min just prior to use. The solutions employed were ca. (5–7)  $\times$  10<sup>-4</sup> M in the organometallic complex and 0.1 M in [n-Bu<sub>4</sub>N]PF<sub>6</sub> and were maintained under an atmosphere of N<sub>2</sub>. Under these conditions, the Cp<sub>2</sub>Fe/[Cp<sub>2</sub>Fe]<sup>+</sup> couple was measured at E<sup>o'</sup> =

(6) Christensen, N. J.; Hunter, A. D.; Legzdins, P. *Organometallics* 1989, 8, 930.

(7) (a) Shriver, D. F.; Drezdson, M. A. *The Manipulation of Air-Sensitive Compounds*, 2nd ed.; Wiley-Interscience: Toronto, 1986. (b) Wayda, A. L.; Darensbourg, M. Y. *Experimental Organometallic Chemistry: A Practicum in Synthesis and Characterization*; ACS Symposium Series 357; American Chemical Society: Washington, DC, 1987.

(8) Perrin, D. D.; Armarego, W. L. F.; Perrin, D. R. *Purification of Laboratory Chemicals*, 2nd ed.; Pergamon Press: Oxford, England, 1980.

(9) Malito, J. T.; Shaker, R.; Atwood, J. L. *J. Chem. Soc., Dalton Trans.* 1980, 1253.

(10) (a) Legzdins, P.; Wassink, B. *Organometallics* 1984, 3, 1811. (b) Herring, F. G.; Legzdins, P.; Richter-Addo, G. B. *Organometallics* 1989, 8, 1485.

Table I.  $^1\text{H}$  and  $^{13}\text{C}$  NMR Properties of the  $\text{Cp}^*\text{Mo}(\text{NO})(\eta^4\text{-trans-}(E)\text{- or -}(Z)\text{-1,3-pentadiene})$  Complexes 1A and 1B in  $\text{C}_6\text{D}_6$ 

1A

1B

$^1\text{H}$ NMR Chemical Shifts ( $\delta$ , ppm)								
complex	Cp*	H <sub>11</sub>	H <sub>12</sub>	H <sub>21</sub>	H <sub>32</sub>	H <sub>41</sub>	H <sub>42</sub>	CH <sub>3</sub>
1A	1.87 (s)	2.43 (dd)	2.85 (dd)	1.51 (m)	3.44 (t)	2.06 (m)		1.90 (s)
1B	1.87 (s)	2.07 (m)		3.44 (t)	1.52 (m)	2.85 (dd)	2.44 (dd)	1.89 (s)

$^1\text{H}$ NMR Coupling Constants ( $J$ , Hz)							
complex	$J_{11-12}$	$J_{11-21}$	$J_{12-21}$	$J_{21-32}$	$J_{32-41}$	$J_{32-42}$	$J_{41-42}$
1A	2.5	6.8	14.4	11.4	11.4		
1B		6.0		11.3	14.1	6.7	2.6

$^{13}\text{C}$ NMR Chemical Shifts [ $\delta$ , ppm ( $^1J_{\text{CH}}$ , Hz)]								
complex	C <sub>5</sub> Me <sub>5</sub>	C <sub>5</sub> Me <sub>5</sub>	C <sub>1</sub>	C <sub>2</sub>	C <sub>3</sub>	C <sub>4</sub>	C <sub>4</sub>	C <sub>Me</sub>
1A	106.35 (s)	10.70 (q) (127.3)	58.50 (t) (158.0)	88.42 (d) (153.2)	99.05 (d) (160.8)	79.51 (d) (148.8)	19.41 (q) (128.0)	
1B	104.52 (s)	10.39 (q) (126.0)	79.45 (d) (152.0)	99.45 (d) (158.0)	88.50 (d) (158.0)	58.51 (t) (156.7)	19.41 (q) (126.7)	

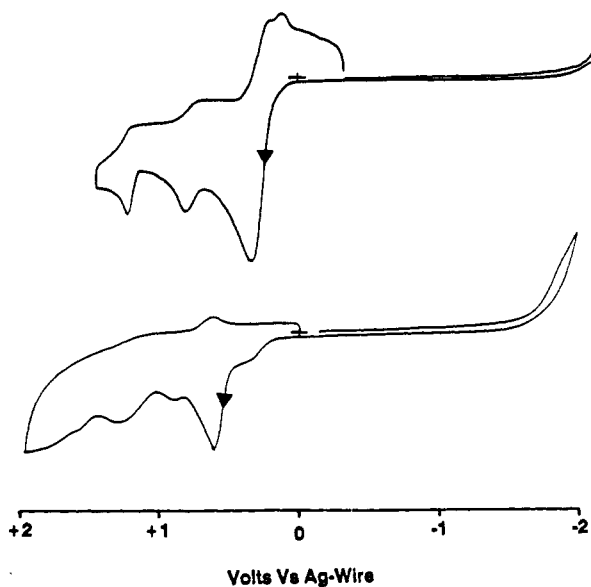


Figure 1. Ambient-temperature cyclic voltammograms of (a)  $\text{CpMo}(\text{NO})(\eta^4\text{-trans-2,5-dimethyl-2,4-hexadiene})$  and (b)  $\text{CpMo}(\text{NO})(\eta^4\text{-cis-2,3-dimethylbutadiene})$  in  $\text{CH}_2\text{Cl}_2$  containing 0.1 M  $[\text{n-Bu}_4\text{N}]\text{PF}_6$  at a scan rate of 110  $\text{mV s}^{-1}$ .

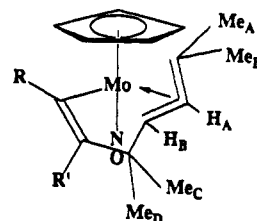
0.46 V versus SCE in  $\text{CH}_2\text{Cl}_2$ , and the ratio of the anodic peak current to cathodic peak current ( $i_{p,a}/i_{p,c}$ )<sup>11</sup> was 1. The cyclic voltammograms of  $\text{CpMo}(\text{NO})(\eta^4\text{-trans-2,5-dimethyl-2,4-hexadiene})$  and  $\text{CpMo}(\text{NO})(\eta^4\text{-cis-2,3-dimethylbutadiene})$  in  $\text{CH}_2\text{Cl}_2$  are presented in Figure 1.

**Reactions of  $\text{CpMo}(\text{NO})(\eta^4\text{-trans-2,5-dimethyl-2,4-hexadiene})$  with 1-Phenylpropyne and 1,7-Octadiyne.** The treatment of  $\text{CpMo}(\text{NO})(\eta^4\text{-trans-2,5-dimethyl-2,4-hexadiene})$  with the two alkynes was effected in a similar manner, and the reaction with 1-phenylpropyne is described below as a representative example.

In a Schlenk tube  $\text{CpMo}(\text{NO})(\eta^4\text{-trans-2,5-dimethyl-2,4-hexadiene})$  (0.30 g, 1.0 mmol) was dissolved in 1-phenylpropyne (2 mL) to produce a brown solution whose IR spectrum exhibited  $\nu_{\text{NO}}$  at 1618  $\text{cm}^{-1}$ . The Schlenk tube was sealed and heated to 50 °C for 12 h. Hexanes (40 mL) were then added, and the solution was filter-cannulated to the top of a Florisil column (3 × 3 cm) made up in hexanes. The excess of alkyne reagent was washed from the column with hexanes and discarded. A second,

yellow band was eluted with  $\text{Et}_2\text{O}$  and collected. The solvent was removed from the eluate under reduced pressure to obtain analytically pure  $\text{CpMo}(\text{NO})[\eta^4\text{-C}(\text{Me})_2\text{CHCHC}(\text{Me})_2\text{C}(\text{Me})\text{C}(\text{Ph})]$  (2) in 70% yield. A crystal suitable for X-ray crystallographic analysis was grown by maintaining a concentrated hexanes solution of 2 at -20 °C for 2 weeks.

Anal. Calcd for  $\text{C}_{29}\text{H}_{27}\text{NOMo}$ : C, 63.34; H, 6.47; N, 3.35. Found: C, 63.36; H, 6.38; N, 3.32. IR (hexanes):  $\nu_{\text{NO}}$  1633  $\text{cm}^{-1}$ . IR (Nujol mull):  $\nu_{\text{NO}}$  1628  $\text{cm}^{-1}$ . [NMR assignments for both alkyne-inserted products are based upon the structure and labeling scheme shown, i.e. in 2, R = Ph and R' = Me<sub>E</sub> and, in 3, R =  $(\text{CH}_2)_4\text{CCH}$  and R' = H.]



Thus, NMR data for 2 are as follows.  $^1\text{H}$  NMR ( $\text{C}_6\text{D}_6$ ):  $\delta$  6.9–7.0 (m, 5 H, C<sub>6</sub>H<sub>5</sub>), 5.43 (dd, 1 H,  $J_{\text{HH}} = 14.0$  Hz, H<sub>A</sub>), 4.78 (s, 5 H, C<sub>2</sub>H<sub>5</sub>), 4.65 (dd, 1 H,  $J_{\text{HH}} = 14.0$  Hz, H<sub>B</sub>), 1.87 (s, 3 H, Me<sub>E</sub>), 1.68 (s, 3 H, Me<sub>D</sub>), 1.24 (s, 3 H, Me<sub>A</sub>), 1.22 (s, 3 H, Me<sub>B</sub>), 1.00 (s, 3 H, Me<sub>C</sub>).  $^{13}\text{C}$  NMR ( $\text{C}_6\text{D}_6$ ):  $\delta$  159.3 (s, =C–Me), 154.9 (s, =C–Ph), 121–131 (m, C<sub>6</sub>H<sub>5</sub>), 110.5 (d,  $^1J_{\text{CH}} = 147$  Hz, CH<sub>A</sub>), 106.3 (d,  $^1J_{\text{CH}} = 147$  Hz, CH<sub>B</sub>), 102.2 (dp,  $^1J_{\text{CH}} = 176$  Hz,  $^2J_{\text{CH}} = 7$  Hz, C<sub>5</sub>H<sub>5</sub>), 69.5 (s, CMe<sub>2</sub>), 47.5 (s, CMe<sub>2</sub>), 29.3 (q,  $^1J_{\text{CH}} = 125.4$  Hz, Me<sub>B</sub>), 29.2 (q,  $^1J_{\text{CH}} = 125.0$  Hz, Me<sub>D</sub>), 26.9 (q,  $^1J_{\text{CH}} = 126.1$  Hz, Me<sub>C</sub>), 25.8 (q,  $^1J_{\text{CH}} = 122.0$  Hz, Me<sub>A</sub>), 18.5 (q,  $^1J_{\text{CH}} = 126.1$  Hz, Me<sub>E</sub>). Low-resolution mass spectrum (probe temperature 120 °C):  $m/z$  419 ( $\text{P}^+$ ,  $^{98}\text{Mo}$ ).

Treatment of  $\text{CpMo}(\text{NO})(\eta^4\text{-trans-2,5-dimethyl-2,4-hexadiene})$  (0.3 g, 1.0 mmol) with 1,7-octadiyne (0.5 g, excess) in hexanes (20 mL) followed by a similar workup procedure led to the isolation of  $\text{CpMo}(\text{NO})[\eta^4\text{-C}(\text{Me})_2\text{CHCHC}(\text{Me})_2\text{CHC}[(\text{CH}_2)_4\text{CCH}]]$  (3) in 60% yield.

Anal. Calcd for  $\text{C}_{21}\text{H}_{29}\text{NOMo}$ : C, 61.94; H, 7.12; N, 3.44. Found: C, 61.73; H, 7.10; N, 3.48. IR (hexanes):  $\nu_{\text{NO}}$  1632  $\text{cm}^{-1}$ . IR (Nujol mull):  $\nu_{\text{NO}}$  1606  $\text{cm}^{-1}$ . Two isomers, arbitrarily designated as A and B, exist in solution in a ratio of A:B = 7:1. (Labeling of H<sub>A</sub> and H<sub>B</sub> is as shown in the labeling scheme.)  $^1\text{H}$  NMR ( $\text{C}_6\text{D}_6$ ) isomer A:  $\delta$  6.32 (s, 1 H, =CH–), 5.35 (d, 1 H,  $J_{\text{HH}} = 14.0$  Hz, H<sub>A</sub>), 4.99 (s, 5 H, C<sub>5</sub>H<sub>5</sub>), 4.72 (d, 1 H,  $J_{\text{HH}} = 14.0$  Hz, H<sub>B</sub>), 2.1–2.4 (m, 5 H,  $(\text{CH}_2)_4\text{CCH}$  × 2), 1.84 (s, 3 H, Me), 1.60–1.83 (m, 4 H,  $(\text{CH}_2)_4\text{CCH}$  × 2), 1.24 (s, 3 H, Me), 1.21 (s, 3 H, Me), 1.01 (s, 3 H, Me).  $^1\text{H}$  NMR ( $\text{C}_6\text{D}_6$ ) isomer B:  $\delta$  6.54 (s, 1 H, =CH), 5.04,

(11) Nicholson, R. S. *Anal. Chem.* 1966, 38, 1406.

Table II. Elemental Analysis and Mass Spectral and Infrared Data for the  $\eta^3$ -Allyl Complexes 4-7

complex	yield, %	analytical data, %			low resolu mass spectral data P <sup>+</sup> , m/z <sup>a</sup>	$\nu_{\text{NO}}$ , cm <sup>-1</sup>	
		C	H	N		CH <sub>2</sub> Cl <sub>2</sub>	Et <sub>2</sub> O
4	95	36.54 (36.41)	4.40 (4.66)	3.07 (3.27)	431	1653	1667
5	77	51.02 (50.75)	6.00 (5.70)	2.69 (2.96)	365	1657	1665
6	61	43.37 (43.40)	4.82 (4.82)	3.27 (3.37)	303	1665	1661
7	98	28.89 (28.98)	3.23 (3.22)	3.68 (3.76)	375	1652	1665

<sup>a</sup> Assignments for <sup>98</sup>Mo.

(d, 1 H,  $J_{\text{HH}} = 14.0$  Hz,  $H_A$ ), 4.61 (d, 1 H,  $J_{\text{HH}} = 14.0$  Hz,  $H_B$ ), 2.1-2.4 (m, 5 H,  $(\text{CH}_2) \times 2$ ,  $\equiv\text{CH}$ ), 1.60-1.83 (m, 4 H,  $(\text{CH}_2) \times 2$ ), 1.55 (s, 3 H, Me), 1.50 (s, 3 H, Me), 1.35 (s, 3 H, Me), 0.85 (s, 3 H, Me).

<sup>13</sup>C NMR (C<sub>6</sub>D<sub>6</sub>) isomer A:  $\delta$  163.1 (s,  $\equiv\text{CH}$ ), 158.0 (d,  $^1J_{\text{CH}} = 144$  Hz,  $\equiv\text{CH}-\text{Mo}$ ), 111.3 (d,  $^1J_{\text{CH}} = 156$  Hz,  $\text{CH}_A$ ), 107.9 (d,  $^1J_{\text{CH}} = 148$  Hz,  $\text{CH}_B$ ), 100.8 (dp,  $^1J_{\text{CH}} = 176$  Hz,  $^2J_{\text{CH}} \approx ^3J_{\text{CH}} = 244$  Hz,  $\text{C}_6\text{H}_5$ ), 85.1 (s,  $\text{CMe}_2$ ), 77.7 (s,  $\text{CMe}_2$ ), 68.6 (d,  $^1J_{\text{CH}} = 244$  Hz,  $\equiv\text{CH}$ ), 66.9 (s,  $\equiv\text{C}-\text{CH}_2$ ), 46.4 (t,  $^1J_{\text{CH}} = 120$  Hz,  $\text{CH}_2$ ), 28.9 (t,  $^1J_{\text{CH}} = 132$  Hz,  $\text{CH}_2$ ), 28.7 (t,  $^1J_{\text{CH}} = 136$  Hz,  $\text{CH}_2$ ), 18.6 (t,  $^1J_{\text{CH}} = 128$  Hz,  $\text{CH}_2$ ), 29.9, 29.1, 27.2, 27.1 (overlapping multiplets, Me  $\times 4$ ). <sup>13</sup>C{<sup>1</sup>H} NMR (C<sub>6</sub>D<sub>6</sub>) isomer B (concentration too low for adequate signal-to-noise in the <sup>13</sup>C NMR spectrum to permit definitive assignments):  $\delta$  162.0, 158.5, 106.3, 100.0, 97.2, 46.7, 43.7, 31.7, 29.6, 29.4, 24.2, 23.9.

Low-resolution mass spectrum (probe temperature 150 °C): m/z 419 (P<sup>+</sup>, <sup>98</sup>Mo).

**Reactions of CpMo(NO)( $\eta^4$ -*trans*-2,5-dimethyl-2,4-hexadiene) with HX (X = I, O<sub>2</sub>CCF<sub>3</sub>, O<sub>3</sub>S-*p*-C<sub>6</sub>H<sub>4</sub>CH<sub>3</sub>).** The reactions of CpMo(NO)( $\eta^4$ -*trans*-2,5-dimethyl-2,4-hexadiene) with the HX species were effected in a similar manner. The reaction with HI is presented below as a representative example.

To a reaction flask containing CpMo(NO)( $\eta^4$ -*trans*-2,5-dimethyl-2,4-hexadiene) (0.30 g, 1.0 mmol) in CH<sub>2</sub>Cl<sub>2</sub> (50 mL) ( $\nu_{\text{NO}}$  1584 cm<sup>-1</sup>) was added aqueous HI (0.25 mL, ca. 1 mmol) by syringe. The color of the solution immediately changed from yellow to red, and an IR spectrum of the solution exhibited a band attributable to  $\nu_{\text{NO}}$  at 1653 cm<sup>-1</sup>. The reaction mixture was stirred for 10 min, and then the solvent was removed under reduced pressure. The remaining orange residue was extracted with Et<sub>2</sub>O (3  $\times$  50 mL), and the red extracts were filter-cannulated to a fresh flask in which the solvent volume was reduced to approximately 70 mL in vacuo. This solution was slowly layered with hexanes and cooled to 0 °C overnight to induce the crystallization of analytically pure CpMo(NO)( $\eta^3$ -C<sub>6</sub>H<sub>15</sub>)I (4) as an orange-red solid.

Physical and analytical data for all the allyl complexes prepared by the reactions of CpMo(NO)( $\eta^4$ -*trans*-2,5-dimethyl-2,4-hexadiene) with HI (4), trifluoroacetic acid (5), and *p*-toluenesulfonic acid (6) are collected in Tables II and III. Also contained in these tables are the data for a similar product complex (7) prepared in a similar manner from the reaction of CpMo(NO)( $\eta^4$ -*trans*-butadiene) with HI.

#### X-ray Crystallographic Analyses of Complexes 1A and 2.

Both X-ray structure determinations were performed in a similar manner after suitable X-ray-quality crystals of each complex had been obtained as described in the preceding paragraphs. Each crystal was mounted in a thin-walled glass capillary under N<sub>2</sub> and transferred to an Enraf-Nonius CAD4-F diffractometer equipped with graphite-monochromated Mo K $\alpha$  radiation ( $\lambda = 0.71069$  Å). The crystals of Cp\*Mo(NO)( $\eta^4$ -*trans*-*E*)-1,3-pentadiene (1A) were cooled to 210 K by using a locally developed apparatus based on a commercial Enraf-Nonius system. Final unit-cell parameters for each complex were obtained by least-squares analysis of  $2(\sin \theta)/\lambda$  values for 25 well-centered high-angle reflections (i.e.  $40^\circ < 2\theta < 48^\circ$  for 1A and  $31^\circ < 2\theta < 43^\circ$  for 2). The intensities of three standard reflections were measured every 9000 s of X-ray exposure time during the data collection of 1A and showed some fluctuation in intensity with time ( $\pm 8.5\%$ ) in blocklike steps. The standard reflections were employed to scale the data for 1A by using a five-point smoothing curve within each block. Two standard reflections for 2 measured every 5400 s showed no appreciable variation with time ( $< 1.1\%$ ). The data for both complexes were corrected for Lorentz and polarization effects, and an analytical absorption correction was applied.<sup>12</sup>

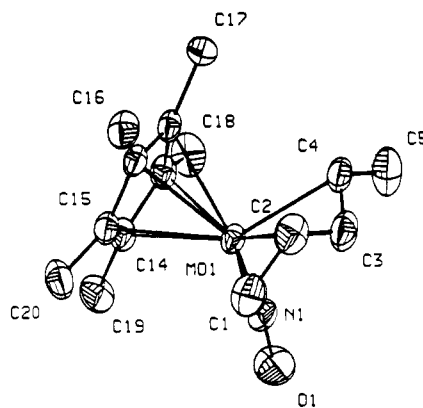


Figure 2. View of the solid-state molecular structure of Cp\*Mo(NO)( $\eta^4$ -*trans*-*E*)-1,3-pentadiene (1A).

Pertinent crystallographic and experimental parameters for 1A and 2 are summarized in Table IV.

The structure of 1A was solved by conventional heavy-atom methods and was refined by full-matrix least squares, minimizing the function  $\sum w(|F_o| - |F_c|)^2$ , where  $w$  was calculated from a three-term Chebyshev series so that  $w = 1/[30.544t_0(x) + 42.072t_1(x) + 12.364t_2(x)]$ , where  $x = F_o - F_{\text{max}}^2$  during the final stages of refinement. Most of the hydrogen atoms were located in difference Fourier maps. Nevertheless, it was decided to place geometrically all the hydrogen atoms except for the vinyl ones, which were left in their observed positions. All hydrogen atoms were then allowed to ride on the atoms to which they were attached, with similar hydrogen atoms being given equivalent temperature factors. All non-hydrogen atoms were given anisotropic thermal parameters.

The structure of 2 was solved by conventional heavy-atom methods and was refined by full-matrix least squares, minimizing the function  $\sum w(|F_o| - |F_c|)^2$ , where  $w$  was calculated from  $w = [(\sigma(F_o))^2 + 0.00025F_o^2]^{-1}$ . One reflection that showed extinction effects (001) was omitted from the refinement. All hydrogen atoms were located in difference Fourier maps and were included in the refinement. The variables included in the refinement of 2 were positional and anisotropic thermal parameters for all the non-hydrogen atoms and positional and individual thermal parameters for the hydrogen atoms.

The final residuals  $R$ ,  $R_w$ , goodness of fit (GOF), and highest residual density for the refinements of complexes 1A and 2 are listed in Table IV. The refinements were considered complete when the ratios of all shifts to esd's were less than 0.1. Complex neutral-atom scattering factors were taken from ref 13. The computations were performed on a MICROVAX II computer using the NRC VAX crystal structure package<sup>14</sup> and the CRYSTALS suite of programs.<sup>15</sup> Final positional and equivalent isotropic thermal parameters ( $U_{\text{eq}} = 1/3 \times \text{trace diagonalized } U$ ) for the complexes 1A and 2 are given in Tables V and VI. Bond lengths

(12) Alcock, N. W. In *Crystallographic Computing*; Ahmed, F. R., Ed.; Munksgaard: Copenhagen, 1969; p 271.

(13) *International Tables for X-ray Crystallography*; Kynoch Press: Birmingham, England 1974; Vol. IV, Tables 2.2B and 2.3.1.

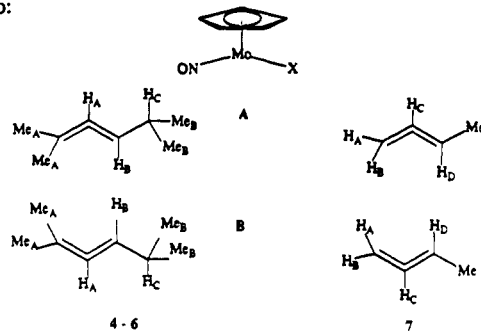
(14) Gabe, E. J.; Larson, A. C.; Lee, F. L.; Le Page, Y. *The NRC VAX Crystal Structure System*; Chemistry Division, National Research Council: Ottawa, Canada, 1984.

(15) Watkin, D. J.; Carruthers, J. R.; Betteridge, P. W. *CRYSTALS User Guide*; Chemical Crystallography Laboratory, University of Oxford: Oxford, U.K., 1985.

Table III.  $^1\text{H}$  NMR Chemical Shifts for the Allyl Complexes 4-7<sup>a</sup>

complex	isomer ratio	isomer A				assgnt	isomer B				
		chem shifts $\delta$ , ppm <sup>b</sup>	multiplicity	integration (no. of H's)	$J$ , Hz		chem shifts $\delta$ , ppm <sup>b</sup>	multiplicity	integration (no. of H's)	$J$ , Hz	assgnt
4	1:0	5.05	s	5		Cp					
		4.12	d	1	10.5	H <sub>A</sub>					
		2.97	d, d	1	10.5, 10.5	H <sub>B</sub>					
		2.30	m	1		H <sub>C</sub>					
		2.21	s	6		Me <sub>A</sub>					
		1.09	d	3	6.5	Me <sub>B</sub>					
		0.99	d	3	6.5	Me <sub>B</sub>					
		5.29	s	5		Cp	5.26	s	5		Cp
5	1.3:1	4.94	d	1	10.5	H <sub>A</sub>	4.32	d	1	10.5	H <sub>A</sub>
		2.32	m	1		H <sub>B</sub>	3.07	d, d	1	10.0, 10.0	H <sub>B</sub>
		1.35	m	1		H <sub>C</sub>	1.35	m	1		H <sub>C</sub>
		1.71	s	3		Me <sub>A</sub>	1.63	s	3		Me <sub>A</sub>
		1.58	s	3		Me <sub>A</sub>	1.09	s	3		Me <sub>A</sub>
		0.95	d	3	6.5	Me <sub>B</sub>	0.91	d	3	6.2	Me <sub>B</sub>
		0.60	d	3	6.5	Me <sub>B</sub>	0.67	d	3	6.5	Me <sub>B</sub>
		5.15	s	5		Cp	5.05	s	5		Cp
6	6:1	4.91	d	1	10.5	H <sub>A</sub>	4.33	d	1	13.0	H <sub>A</sub>
		3.76	d, d	1	9.8, 10.5	H <sub>B</sub>	3.25	d, d	1	9.0, 9.0	H <sub>B</sub>
		2.36	m	1		H <sub>C</sub>	2.36	m	1		H <sub>C</sub>
		1.45	s	3		Me <sub>A</sub>	1.64	s	3		Me <sub>A</sub>
		1.10	s	3		Me <sub>A</sub>	1.59	s	3		Me <sub>A</sub>
		1.05	d	3	6.3	Me <sub>B</sub>	0.95	d	3	6.4	Me <sub>B</sub>
		0.75	d	3	6.3	Me <sub>B</sub>	0.64	d	3	6.3	Me <sub>B</sub>
		5.88	s	5		Cp	5.78	s	5		Cp
7 <sup>c</sup>	4:1	5.04	m	1		H <sub>C</sub>	4.62	m	2		H <sub>A</sub> , H <sub>C</sub>
		4.95	m	1		H <sub>A</sub>	3.45	d, d	1	2.5, 9.0	H <sub>D</sub>
		3.31	d	1	3.0, 6.5	H <sub>D</sub>	2.61	m	1		H <sub>B</sub>
		2.47	d	3	6.3	Me	2.55	d	3	5.5	Me
		2.35	m	1		H <sub>B</sub>					

<sup>a</sup> Labeling scheme for the allyl complexes 4-7, showing the orientation of the allyl ligands with respect to the cyclopentadienyl ligand of the CpMo(NO)X fragment shown at the top:



<sup>b</sup> C<sub>6</sub>D<sub>6</sub>, unless otherwise specified. <sup>c</sup> CDCl<sub>3</sub>.

(Å) and bond angles (deg) for both nitrosyl complexes are listed in Tables VII and VIII, respectively. Anisotropic thermal parameters, the remaining molecular dimensions (including hydrogen atom coordinates), and tables of calculated and observed structure factors for both complexes are provided as supplementary material. Views of the solid-state molecular structures of Cp\*Mo(NO)( $\eta^4$ -*trans*-(*E*)-1,3-pentadiene) (1A) and CpMo(NO)[ $\eta^4$ -C(Me)<sub>2</sub>CHCHC(Me)<sub>2</sub>C(Me)C(Ph)] (2) are presented in Figures 2 and 3, respectively.<sup>16</sup>

## Results and Discussion

**Preparation and Characterization of Cp\*Mo(NO)( $\eta^4$ -*trans*-1,3-pentadiene) Complexes.** The title complexes are preparable in a manner analogous to that summarized in eq 1 in the Introduction of this paper, i.e.

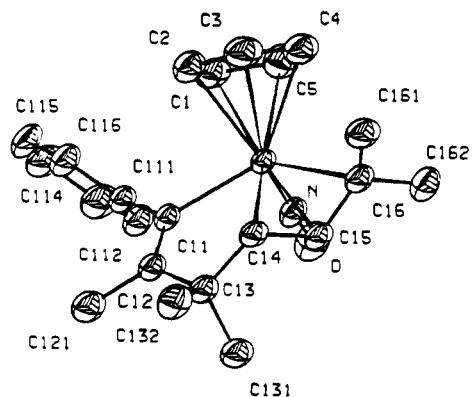
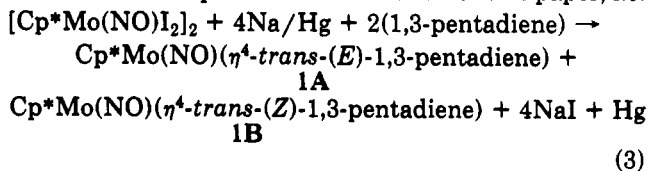


Figure 3. View of the solid-state molecular structure of CpMo(NO)[ $\eta^4$ -C(Me)<sub>2</sub>CHCHC(Me)<sub>2</sub>C(Me)C(Ph)] (2).

This chemical transformation is deserving of special comment because two isomers of Cp\*Mo(NO)( $\eta^4$ -*trans*-1,3-pentadiene), one yellow and one red, may be isolated separately by chromatography on Florisil when the reduction of [Cp\*Mo(NO)I<sub>2</sub>]<sub>2</sub> is effected in the presence of an isomeric mixture of (*E*)- and (*Z*)-1,3-pentadiene. The

**Table IV. Crystallographic and Experimental Data<sup>a</sup> for the Complexes Cp\*Mo(NO)( $\eta^4$ -trans-(*E*)-1,3-pentadiene) (1A) and CpMo(NO)[ $\eta^4$ -C(Me)<sub>2</sub>CHCHC(Me)<sub>2</sub>C(Me)C(Ph)] (2)**

	complex	
	1A	2
formula	C <sub>15</sub> H <sub>23</sub> NOMo	C <sub>22</sub> H <sub>27</sub> NOMo
fw	329.29	417.40
cryst system	monoclinic	triclinic
space group	P2 <sub>1</sub> /c	P1
a, Å	7.312 (1)	7.973 (2)
b, Å	14.535 (3)	9.330 (1)
c, Å	14.602 (5)	14.324 (2)
α, deg		73.04 (1)
β, deg	103.38 (2)	89.33 (2)
γ, deg		72.96 (2)
V, Å <sup>3</sup>	1509.78	971.27
Z	4	2
d <sub>calc</sub> , Mg/m <sup>3</sup>	1.449	1.4273
μ(Mo Kα), cm <sup>-1</sup>	8.375	6.67
T, K	210	295
cryst dimens, mm <sup>3</sup>	0.18 × 0.29 × 0.30	0.35 × 0.39 × 0.16
Mo Kα radiation λ, Å	0.71069	0.71069
transm factors	0.7931–0.8566	0.8040–0.9026
scan mode	coupled ω–2θ	coupled ω–2θ
scan range, deg	1.00 + 0.35 tan θ	1.00 + 0.35 tan θ
scan speed, deg/min	0.82–2.75	0.87–3.30
2θ limits, deg	0 < 2θ ≤ 53	2 < 2θ ≤ 50
data collcd	h, k, ±l	h, ±k, ±l
no. of unique reflcns	2948	3409
no. of reflcns with I > 3σ(I)	2229	2976
no. of variables	165	334
R <sub>F</sub> <sup>b</sup>	0.046	0.018
R <sub>wF</sub> <sup>c</sup>	0.057	0.024
goodness of fit <sup>d</sup>	1.0487	1.157
max Δ/σ (final cycle)	0.1	0.1
resid density, e/Å <sup>3</sup>	2.48 (10) <sup>e</sup>	0.28 (4) <sup>f</sup>

<sup>a</sup> Enraf-Nonius CAD4-F diffractometer, Mo Kα radiation, graphite monochromator. <sup>b</sup> R<sub>F</sub> = Σ||F<sub>o</sub>| – |F<sub>c</sub>|| / Σ|F<sub>o</sub>|. <sup>c</sup> R<sub>wF</sub> = [Σ(|F<sub>o</sub>| – |F<sub>c</sub>||)<sup>2</sup> / Σ|F<sub>o</sub>|<sup>2</sup>]<sup>1/2</sup>. <sup>d</sup> GOF = [Σw(|F<sub>o</sub>| – |F<sub>c</sub>||)<sup>2</sup> / (no. of degrees of freedom)]<sup>1/2</sup>. <sup>e</sup> Situated 0.829 Å from the molybdenum atom. <sup>f</sup> Situated 1.125 Å from the molybdenum atom.

**Table V. Final Positional (×10<sup>4</sup>) and Equivalent Isotropic Thermal Parameters (Å<sup>2</sup> × 10<sup>4</sup>) for Cp\*Mo(NO)( $\eta^4$ -trans-(*E*)-1,3-pentadiene) (1A)**

atom	x/a	y/b	z/c	U <sub>eq</sub>
Mo(1)	368.5 (5)	992.8 (2)	2130.9 (3)	262
N(1)	–936 (6)	–37 (3)	2059 (3)	360
O(1)	–1583 (7)	–810 (3)	2014 (3)	533
C(1)	–1790 (8)	1731 (4)	931 (4)	532
C(2)	–1542 (7)	2182 (4)	1787 (4)	436
C(3)	–1976 (7)	1726 (4)	2572 (4)	443
C(4)	–568 (7)	1616 (4)	3401 (4)	395
C(5)	–814 (10)	1065 (5)	4214 (3)	652
C(11)	3062 (6)	1794 (3)	1868 (3)	278
C(12)	3488 (6)	1515 (3)	2819 (3)	275
C(13)	3418 (6)	532 (3)	2850 (3)	297
C(14)	2998 (6)	204 (3)	1904 (3)	304
C(15)	2741 (6)	983 (3)	1297 (3)	309
C(16)	3113 (7)	2752 (3)	1505 (4)	383
C(17)	4076 (7)	2136 (3)	3669 (3)	370
C(18)	3887 (8)	–60 (4)	3720 (4)	453
C(19)	2965 (8)	–777 (3)	1596 (4)	420
C(20)	2435 (8)	956 (4)	237 (3)	437

physical and analytical data for these complexes, the yellow one being designated 1A and the red 1B, indicate that they have very similar physical properties (Table I).

A crystal of 1A has been subjected to an X-ray crystallographic analysis, and the results of that analysis are presented in Figure 2 and Tables IV–VIII. The complex possesses a type of three-legged piano-stool molecular structure whose intramolecular dimensions generally resemble those extant in CpMo(NO)( $\eta^4$ -trans-2,5-di-

**Table VI. Final Positional and Equivalent Isotropic Thermal Parameters (Å<sup>2</sup>) for CpMo(NO)[ $\eta^4$ -C(Me)<sub>2</sub>CHCHC(Me)<sub>2</sub>C(Me)C(Ph)] (2)**

atom	x/a	y/b	z/c	B <sub>eq</sub> <sup>a</sup>
Mo	0.346 319 (20)	0.404 627 (18)	0.222 613 (11)	2.265
O	0.579 77 (25)	0.573 60 (20)	0.107 73 (14)	5.43
N	0.489 02 (22)	0.506 13 (19)	0.158 71 (12)	3.01
C(1)	0.267 20 (30)	0.301 12 (29)	0.105 57 (17)	3.93
C(2)	0.213 55 (30)	0.219 95 (30)	0.194 05 (19)	4.08
C(3)	0.081 58 (31)	0.326 94 (34)	0.224 63 (21)	4.75
C(4)	0.051 85 (32)	0.475 79 (34)	0.155 05 (21)	4.52
C(5)	0.164 86 (33)	0.458 31 (32)	0.081 53 (18)	4.13
C(11)	0.577 05 (24)	0.191 00 (21)	0.276 49 (13)	2.54
C(12)	0.664 20 (25)	0.145 18 (23)	0.364 49 (14)	2.78
C(13)	0.606 03 (26)	0.257 16 (24)	0.431 38 (14)	2.84
C(14)	0.423 20 (25)	0.353 74 (23)	0.390 06 (14)	2.78
C(15)	0.379 47 (26)	0.513 78 (24)	0.344 29 (14)	2.95
C(16)	0.211 66 (27)	0.602 34 (24)	0.295 74 (15)	3.23
C(111)	0.643 41 (25)	0.108 31 (22)	0.202 41 (14)	2.67
C(112)	0.735 43 (30)	0.173 01 (28)	0.126 64 (17)	3.56
C(113)	0.789 86 (35)	0.102 65 (33)	0.054 40 (19)	4.49
C(114)	0.754 11 (34)	–0.031 78 (35)	0.054 97 (20)	4.89
C(115)	0.667 59 (34)	–0.101 03 (31)	0.130 24 (22)	4.91
C(116)	0.613 39 (31)	–0.031 68 (27)	0.203 86 (18)	3.77
C(121)	0.828 52 (36)	0.005 73 (34)	0.397 53 (21)	4.08
C(131)	0.736 48 (31)	0.340 68 (31)	0.430 01 (19)	3.83
C(132)	0.598 01 (38)	0.153 53 (32)	0.538 04 (17)	3.92
C(161)	0.048 92 (32)	0.580 98 (35)	0.347 21 (20)	4.17
C(162)	0.186 90 (37)	0.769 98 (28)	0.234 02 (21)	4.05

<sup>a</sup> B<sub>eq</sub> is the arithmetic mean of the principal axes of the thermal ellipsoid.

**Table VII. Bond Lengths (Å) with Esd's in Parentheses for 1A and 2**

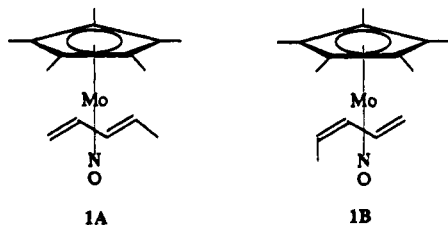
1a			
Mo(1)–N(1)	1.765 (4)	C(3)–C(4)	1.405 (8)
Mo(1)–C(1)	2.331 (5)	C(4)–C(5)	1.476 (8)
Mo(1)–C(2)	2.206 (5)	C(11)–C(12)	1.411 (6)
Mo(1)–C(3)	2.236 (5)	C(11)–C(15)	1.432 (6)
Mo(1)–C(4)	2.306 (5)	C(11)–C(16)	1.493 (6)
Mo(1)–C(11)	2.394 (4)	C(12)–C(13)	1.431 (6)
Mo(1)–C(12)	2.393 (4)	C(12)–C(17)	1.514 (6)
Mo(1)–C(13)	2.332 (4)	C(13)–C(14)	1.426 (6)
Mo(1)–C(14)	2.327 (4)	C(13)–C(18)	1.507 (6)
Mo(1)–C(15)	2.338 (4)	C(14)–C(15)	1.423 (6)
N(1)–O(1)	1.215 (5)	C(14)–C(19)	1.493 (6)
C(1)–C(2)	1.386 (8)	C(15)–C(20)	1.513 (6)
C(2)–C(3)	1.422 (8)		
2			
Mo(1)–N(1)	1.769 (2)	C(11)–C(111)	1.492 (3)
Mo(1)–C(1)	2.338 (2)	C(12)–C(13)	1.517 (3)
Mo(1)–C(2)	2.397 (2)	C(12)–C(121)	1.513 (3)
Mo(1)–C(3)	2.442 (2)	C(13)–C(14)	1.514 (3)
Mo(1)–C(4)	2.378 (2)	C(13)–C(131)	1.538 (3)
Mo(1)–C(5)	2.341 (2)	C(13)–C(132)	1.534 (3)
Mo(1)–C(11)	2.222 (2)	C(14)–C(15)	1.382 (3)
Mo(1)–C(14)	2.357 (2)	C(15)–C(16)	1.412 (3)
Mo(1)–C(15)	2.313 (2)	C(16)–C(161)	1.520 (3)
Mo(1)–C(16)	2.365 (2)	C(16)–C(162)	1.511 (3)
O(1)–N(1)	1.200 (2)	C(111)–C(112)	1.393 (3)
C(1)–C(2)	1.407 (4)	C(111)–C(116)	1.389 (3)
C(1)–C(5)	1.395 (4)	C(112)–C(113)	1.382 (3)
C(2)–C(3)	1.387 (4)	C(113)–C(114)	1.363 (4)
C(3)–C(4)	1.408 (4)	C(114)–C(115)	1.376 (4)
C(4)–C(5)	1.393 (4)	C(115)–C(116)	1.393 (3)
C(11)–C(12)	1.337 (3)		

methyl-2,4-hexadiene).<sup>4</sup> For instance, the carbon–carbon bond lengths among the four coordinated carbons of the diene ligand in 1A are approximately equivalent, a feature consistent with the bonding rationale currently invoked for all the Cp\*Mo(NO)( $\eta^4$ -trans-diene) (Cp' = Cp or Cp\*) complexes isolated to date (vide infra).<sup>6</sup> The most significant feature of the molecular structure of 1A is the fact that the transoidal (*E*)-1,3-pentadiene ligand is coordinated to the molybdenum with its methyl substituent pointing

Table VIII. Bond Angles (deg) with Esd's in Parentheses for 1A and 2

1a			
C(1)-Mo(1)-N(1)	94.8 (2)	C(3)-C(4)-Mo(1)	69.3 (3)
C(2)-Mo(1)-N(1)	110.3 (2)	C(5)-C(4)-Mo(1)	123.2 (4)
C(2)-Mo(1)-C(1)	35.4 (2)	C(5)-C(4)-C(3)	123.6 (5)
C(3)-Mo(1)-N(1)	89.0 (2)	C(15)-C(11)-C(12)	107.8 (4)
C(3)-Mo(1)-C(1)	64.3 (2)	C(16)-C(11)-C(12)	126.9 (4)
C(3)-Mo(1)-C(2)	37.3 (2)	C(16)-C(11)-C(15)	125.1 (4)
C(4)-Mo(1)-N(1)	97.1 (2)	C(13)-C(12)-C(11)	108.5 (4)
C(4)-Mo(1)-C(1)	98.5 (2)	C(17)-C(12)-C(11)	126.3 (4)
C(4)-Mo(1)-C(2)	65.5 (2)	C(17)-C(12)-C(13)	125.1 (4)
C(4)-Mo(1)-C(3)	36.0 (2)	C(14)-C(13)-C(12)	107.7 (4)
O(1)-N(1)-Mo(1)	170.4 (4)	C(18)-C(13)-C(12)	126.5 (4)
C(2)-C(1)-Mo(1)	67.4 (3)	C(18)-C(13)-C(14)	125.5 (4)
C(1)-C(2)-Mo(1)	77.2 (3)	C(15)-C(14)-C(13)	107.7 (4)
C(3)-C(2)-Mo(1)	72.5 (3)	C(19)-C(14)-C(13)	126.6 (4)
C(3)-C(2)-C(1)	120.0 (5)	C(19)-C(14)-C(15)	125.5 (4)
C(2)-C(3)-Mo(1)	70.2 (3)	C(17)-C(15)-C(11)	108.2 (4)
C(4)-C(3)-Mo(1)	74.7 (3)	C(20)-C(15)-C(11)	125.6 (4)
C(4)-C(3)-C(2)	119.5 (5)	C(20)-C(15)-C(14)	125.7 (4)
2			
C(11)-Mo(1)-N(1)	88.8 (1)	C(131)-C(13)-C(14)	111.9 (2)
C(14)-Mo(1)-N(1)	105.6 (1)	C(132)-C(13)-C(12)	113.7 (2)
C(14)-Mo(1)-C(11)	69.1 (1)	C(132)-C(13)-C(14)	109.0 (2)
C(15)-Mo(1)-N(1)	85.6 (1)	C(132)-C(13)-C(131)	108.0 (2)
C(15)-Mo(1)-C(11)	96.1 (1)	C(13)-C(14)-Mo(1)	117.9 (1)
C(15)-Mo(1)-C(14)	34.4 (1)	C(15)-C(14)-Mo(1)	71.1 (1)
C(16)-Mo(1)-N(1)	94.0 (1)	C(15)-C(14)-C(13)	125.2 (2)
C(16)-Mo(1)-C(11)	130.4 (1)	C(14)-C(15)-Mo(1)	74.5 (1)
C(16)-Mo(1)-C(14)	62.4 (1)	C(16)-C(15)-Mo(1)	74.5 (1)
C(16)-Mo(1)-C(15)	35.1 (1)	C(16)-C(15)-C(14)	122.1 (2)
O(1)-N(1)-Mo(1)	174.0 (2)	C(15)-C(16)-Mo(1)	70.4 (1)
C(5)-C(1)-C(2)	107.6 (2)	C(161)-C(16)-Mo(1)	114.1 (1)
C(3)-C(2)-C(1)	108.3 (2)	C(161)-C(16)-C(15)	119.0 (2)
C(4)-C(3)-C(2)	107.9 (2)	C(162)-C(16)-Mo(1)	116.3 (1)
C(5)-C(4)-C(3)	107.8 (2)	C(162)-C(16)-C(15)	117.8 (2)
C(4)-C(5)-C(1)	108.4 (2)	C(162)-C(16)-C(161)	112.8 (2)
C(12)-C(11)-Mo(1)	124.2 (1)	C(112)-C(111)-C(11)	120.1 (2)
C(111)-C(11)-Mo(1)	114.8 (1)	C(116)-C(111)-C(11)	122.5 (2)
C(111)-C(11)-C(12)	120.6 (2)	C(116)-C(111)-C(112)	117.4 (2)
C(13)-C(12)-C(11)	118.3 (2)	C(113)-C(112)-C(111)	121.0 (2)
C(121)-C(12)-C(11)	123.6 (2)	C(114)-C(113)-C(112)	120.9 (3)
C(121)-C(12)-C(13)	117.8 (2)	C(115)-C(114)-C(113)	119.5 (2)
C(14)-C(13)-C(12)	105.5 (2)	C(116)-C(115)-C(114)	120.0 (2)
C(131)-C(13)-C(12)	108.8 (2)	C(115)-C(116)-C(111)	121.1 (2)

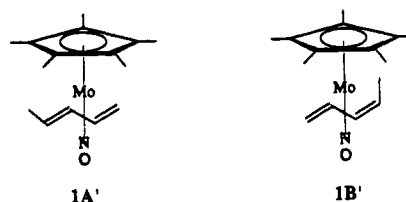
away from the cyclopentadienyl ring. Regrettably, repeated attempts to obtain crystals of **1B** suitable for a similar X-ray structural analysis have to date been unsuccessful. However, the NMR data for **1B** are consistent with its formulation as Cp\*Mo(NO)( $\eta^4$ -*trans*-(*Z*)-1,3-pentadiene), i.e.



The  $^1\text{H}$  NMR spectral data for **1A** and **1B** in  $\text{CDCl}_3$  are presented in Table I and illustrate that the two complexes exhibit only slight differences in their chemical shifts and coupling patterns. [The H substituents in Table I are numbered such that their second digits indicate whether the couplings listed are *cis* (same second digit) or *trans* (different second digit). The same first digits indicate that a *gem* coupling is being specified.] Most notably, the chemical shifts of the resonances due to the methyl hydrogens of the diene ligands are virtually identical (**1A**, 1.90 ppm; **1B**, 1.89 ppm), thereby indicating that the methyl group of each isomer is probably in a similar en-

vironment, i.e. both pointing away from the Cp\* ligand. Consistent with this conclusion are the  $^1\text{H}$ - $^1\text{H}$  coupling constants evident in the  $^1\text{H}$  NMR spectra of both complexes (Table I). For **1A**, it is expected, and found, that three *trans*  $^1\text{H}$ - $^1\text{H}$  couplings ( $J_{12-21}$ ,  $J_{21-32}$ ,  $J_{32-41}$ ) and one *cis*  $^1\text{H}$ - $^1\text{H}$  coupling ( $J_{11-21}$ ) are observable, while, for **1B**, two *trans*  $^1\text{H}$ - $^1\text{H}$  couplings ( $J_{21-32}$ ,  $J_{32-41}$ ) and two *cis*  $^1\text{H}$ - $^1\text{H}$  couplings ( $J_{11-21}$ ,  $J_{32-42}$ ) are evident. The magnitudes of these couplings also fall in the ranges of  $^3J_{\text{HH}}$  values generally observed for these types of compounds, i.e.  $^3J_{\text{trans}} = 10\text{--}15$  Hz and  $^3J_{\text{cis}} = 5\text{--}8$  Hz.<sup>6</sup> In addition, the fact that **1A** and **1B** in a variety of solvents exhibit identical nitrosyl-stretching frequencies in their IR spectra is also most consistent with (but not definitive proof of) both complexes possessing *trans*-diene ligands.

One aspect about the formation of **1A** and **1B** from transformation (3) is worthy of note. It is interesting that no isomers of **1A** and **1B** are detectable spectroscopically in solutions of these complexes. By analogy with other Cp\*Mo(NO)( $\eta^4$ -*trans*-diene) compounds,<sup>6</sup> it might be expected that both **1A** and **1B** would exist in equilibrium in solution with their corresponding diastereomers, **1A'** and **1B'**, i.e.



in which the diene ligand has the opposite face bound to the metal. While it is possible that the other diastereomers are simply not formed during reaction 3, it is more likely that they are present in only very small quantities and hence are not detectable. In any event, it is clear from these studies that even though the Cp\*Mo(NO) fragment in **1A** and **1B** exerts the electronic influence to bind the diene ligands in a twisted, transoidal fashion, steric interactions determine which face of the diene ligand can best accommodate this electronic requirement. In terms of their physical properties, however, it is remarkable that **1A** and **1B** are such distinctly different complexes that may be separated by chromatography on a Florisil column.<sup>6</sup>

**Electrochemical Studies of CpMo(NO)( $\eta^4$ -diene) Complexes.** In order to better understand the reactivity of the  $\eta^4$ -*cis*- and  $\eta^4$ -*trans*-diene complexes, electrochemical studies have been carried out on two representative compounds, namely CpMo(NO)( $\eta^4$ -*trans*-2,5-dimethyl-2,4-hexadiene) and CpMo(NO)( $\eta^4$ -*cis*-2,3-dimethylbutadiene), whose syntheses and characterization we have reported previously.<sup>6</sup> The cyclic voltammograms of these two complexes in  $\text{CH}_2\text{Cl}_2$  are shown in Figure 1.

The cyclic voltammograms indicate that both diene-containing complexes are reasonably stable with respect to reduction, since no reduction behavior is observable to the solvent limit (ca.  $-2$  V). This observation is consistent with the view that each of these complexes has a large HOMO-LUMO energy gap, as demonstrated by Fenske-Hall molecular orbital calculations on the CpMo(NO)( $\eta^4$ -butadiene) model systems.<sup>5</sup> Since the compounds are formed and isolated under highly reducing conditions (i.e. in the presence of Na/Hg), this stability to electron addition is not a surprising result. The fact that the *trans*-diene complex reacts rather reluctantly with Lewis bases such as phosphines<sup>6</sup> may also be partially explained on the basis of this result, since it has been suggested that some such reactions may proceed via initial electron transfer rather than simple nucleophilic displacement.<sup>17</sup>

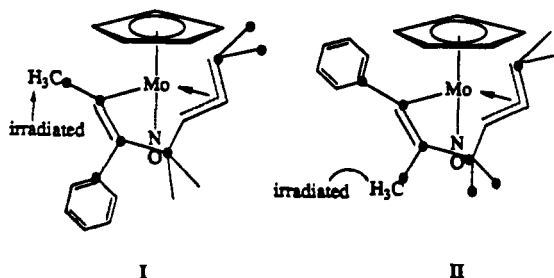




tained for the 1-phenylpropyne coupled complex, 2, is outlined below. The 2D-HETCOR NMR spectrum of 2 is presented in Figure 4. From the 1D  $^1\text{H}$  and  $^{13}\text{C}$  and the 2D-HETCOR NMR spectra, the proton resonances may be assigned to their respective  $^1J$  carbon resonances.

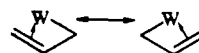
The SINEPT NMR spectrum obtained when the AB-type proton resonance at 5.41 ppm is irradiated is shown in Figure 5a.<sup>20</sup> It is evident that this irradiation causes a polarization transfer to be observed for several carbons. Signal enhancement is observed for the carbon due to the other CH fragment, the cyclopentadienyl ring carbons, each of the end carbons of what was once the diene ligand ( $\text{CMe}_2$ ), and two methyl carbons. Figure 5b shows that irradiation of the AB proton that resonates at 4.62 ppm enhances the signals due to the Cp ring carbons, the  $\text{CMe}_2$  carbons, and two methyl carbons in addition to the carbon of the other CH fragment. While these two experiments do not by themselves establish the coupling of the diene with the alkyne in the metal's coordination sphere, there is an interesting observation to be made at this point. It is notable that the polarization transfer is seen for the cyclopentadienyl ring carbons. This observation means that the polarization transfer has occurred through molybdenum-carbon bonds. This is a phenomenon that, to the best of our knowledge, has not been previously documented in the literature.

The experiment that unambiguously establishes that the coupling reaction shown in eq 4 has indeed occurred is that in which the resonance due to the methyl protons at 1.87 ppm in the proton NMR spectrum is irradiated just downfield of this resonance to ensure that the other methyl group signals are not being weakly irradiated. This spectrum is shown in Figure 5c. Enhancement of the signals at 159.3 and 154.9 ppm is clearly evident. In addition, enhancement of the signals due to both of the  $\text{CMe}_2$  carbons is observed, this probably being the most important effect seen in this experiment. In other words, the methyl proton resonance that was irradiated is that due to the methyl group of the alkyne fragment. Irradiation of this signal is expected to enhance the signals due to the olefinic carbons. If the structure of the product complex involved an  $\eta^2$ -acetylene-metal linkage (i.e. structure A), enhancement of perhaps one of the  $\text{CMe}_2$  signals may be expected, since it is known that the polarization transfer may go through the molybdenum. That effect would be one that was passed through four bonds. In order to see the enhancement of the signal due to the other  $\text{CMe}_2$  carbon, the transfer would need to occur through six bonds, which is beyond the sensitivity of the experiment. In agreement with the conclusion that a coupling reaction has occurred is the observed enhancement of only two methyl carbon signals (in addition to a signal for the carbon to which the irradiated protons are bonded). The net conclusion from the NMR studies is that complex 2 possesses one of molecular structures I or II, the carbons that exhibit the enhanced signals upon irradiation of the methyl proton resonance being designated by black dots. The SINEPT experiments imply that II is more likely than I, since this decreases the average number of bonds between the irradiated protons and the enhanced carbons. In this fashion, then, it is possible to determine the molecular structures of compounds of this type by using NMR spectroscopy alone. To confirm the conclusions drawn from the NMR analyses, an X-ray crystallographic analysis of complex 2



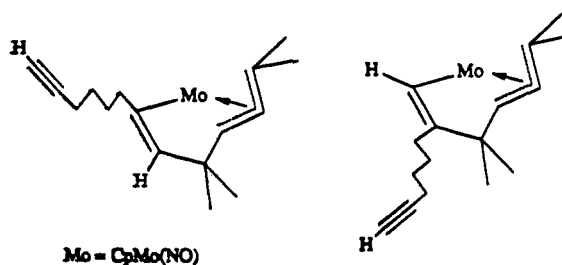
was undertaken.

**X-ray Crystallographic Analysis of Complex 2.** The single-crystal X-ray crystallographic analysis of 2 (the essential details of which are summarized in Table IV) has established that this organometallic complex is a coordinatively saturated, 18-valence-electron compound. The SNOOPI plot of the molecular structure is shown in Figure 3, and selected bond lengths and bond angles are tabulated in Tables VII and VIII. The SNOOPI plot confirms the coupling reaction of the bound diene and the alkyne to form a  $\eta^4$  ( $\eta^3, \eta^1$ ) ligand in which the  $\eta^3$ -allyl portion of the ligand is oriented endo with respect to the cyclopentadienyl ring. Additional interesting structural features include the similar carbon-carbon bond lengths exhibited by the ally carbons (C(16)-C(15), C(15)-C(14)), which are intermediate between that expected for a carbon-carbon single bond (e.g. C(14)-C(13), C(13)-C(12)) and a carbon-carbon double bond (e.g. C(12)-C(11)). These features may be compared to those found for the allyl ligand in  $\text{CpW}(\text{NO})(\eta^3\text{-C}_3\text{H}_5)$  (X = I,<sup>19b</sup> Cl<sup>19c</sup>) in which the allyl linkage is asymmetrically ( $\sigma, \pi$ ) bound to the metal, i.e.



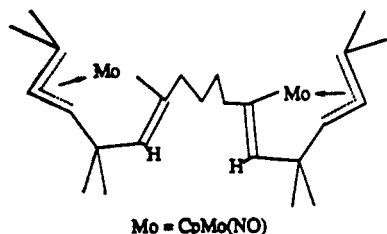
An intriguing feature of the molecular structure is the fact that the alkyne has inserted into the molybdenum-diene-carbon bond so as to position the bulky phenyl group of the alkyne on the carbon nearer to the molybdenum and the cyclopentadienyl ring (i.e. structure II as determined by the SINEPT experiments). This is undoubtedly due to steric interaction between the phenyl group and the methyl groups on the end of the diene ligand, which has been coupled to the alkyne. Molecular models of this complex illustrate that while the phenyl group may orient itself so as to minimize conflict with the cyclopentadienyl ligand when it is attached to the carbon nearest to the molybdenum, the possibilities for such orientation are more limited when the phenyl group is nearer to the two methyl groups, and avoidance of contact with the methyl groups usually results in contact with the cyclopentadienyl ligand.

(b) **1,7-Octadiyne.** The analysis of the NMR spectra exhibited by 3, produced in the reaction between  $\text{CpMo}(\text{NO})(\eta^4\text{-trans-2,5-dimethyl-2,4-hexadiene})$  and 1,7-octadiyne, may be effected in a manner analogous to that outlined for 2 above, but the process is made more difficult by the presence of a second isomer in solution. The probable structures of the two isomers are



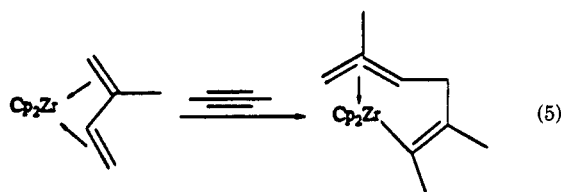
(20) The delay periods used in the pulse sequence of the experiment were not adjusted quite correctly, and this accounts for the signal enhancement seen at 106 ppm for the carbon only one bond away from the irradiated proton.

in which the alkyne-coupled product has the dangling alkyl group either on the carbon bonded to the diene fragment or on the carbon bonded to the molybdenum. By analogy to 2, it is expected that the major isomer is the one in which the dangling alkyl group is attached to the carbon bonded to the molybdenum. The isomers do not interconvert in solution but maintain the ratio in which they are formed. That ratio is always in favor of the same isomer but varies from reaction to reaction. This complex is interesting and leaves one to wonder if it will react with a molecule of CpMo(NO)( $\eta^4$ -*trans*-2,5-dimethyl-2,4-hexadiene) to couple again, i.e.

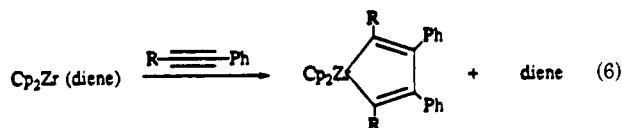


The feasibility of this latter transformation remains to be ascertained.

The reactivity of these molybdenum diene complexes may be compared to that exhibited by the Cp<sub>2</sub>Zr( $\eta^4$ -*trans*-diene) compounds, which has been extensively studied. In the zirconium systems, experimental conditions may be controlled such that the reacting species (i.e.  $\eta^4$ -*cis*-diene or  $\eta^4$ -*trans*-diene) is known. The zirconocene complex, Cp<sub>2</sub>Zr( $\eta^4$ -*trans*-isoprene), reacts with 2-butyne to form the  $\eta^4$  ( $\sigma$ ,  $\eta^3$ )-*syn*-allyl complex as depicted in eq 5.<sup>21</sup> The alkyne always couples with the diene at the

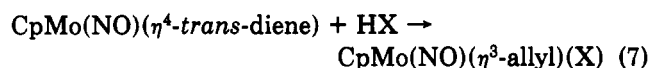


carbon furthest from the methyl substituent of the diene ligand. This product is very similar to those produced during the reactions of alkynes with CpMo(NO)( $\eta^4$ -*trans*-2,5-dimethyl-2,4-hexadiene). In the zirconocene systems, if the alkyne is substituted with a bulky group (e.g. phenyl), the product of the reaction is the metalla-cyclopentadiene complex in which the two alkynes have coupled and the diene ligand has been released,<sup>22</sup> i.e. eq 6. There is no evidence for the formation of these me-



tallacyclic types of products in the molybdenum systems. Evidently, the fact that the molybdenum diene complexes are much less substitutionally labile than their zirconium analogues results in their exhibiting cleaner transformations when treated with acetylenes.

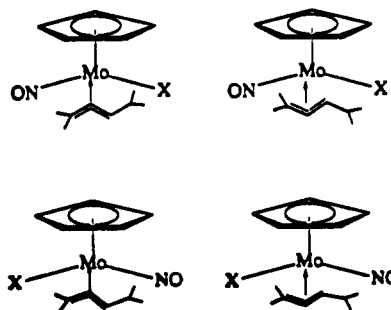
**Reactions of CpMo(NO)( $\eta^4$ -*trans*-diene) Complexes with Protonic Acids HX.** The products of the reactions between CpMo(NO)( $\eta^4$ -*trans*-diene) and HX are the  $\eta^3$ -allyl complexes CpMo(NO)( $\eta^3$ -allyl)(X) i.e. eq 7. Reac-



tions 7 are virtually instantaneous upon mixing of the reagents and proceed cleanly in dichloromethane. The analytical data for the allyl complexes obtained from the reactions between the 2,5-dimethyl-2,4-hexadiene complex and HI (4), HO<sub>3</sub>SC<sub>6</sub>H<sub>4</sub>CH<sub>3</sub> (5), and HO<sub>2</sub>CCF<sub>3</sub> (6) and between the butadiene complex and HI (7) are collected in Tables II and III. Compounds 4–7 are quite soluble in CH<sub>2</sub>Cl<sub>2</sub>, Et<sub>2</sub>O, and THF and not very soluble in hexanes, and thus they can be recrystallized from Et<sub>2</sub>O/hexanes. They are red-orange microcrystalline solids that may be handled in air for short periods of time with no deleterious effects. The analytical and physical data for 4–7 are consistent with their possessing 18-electron three-legged piano-stool molecular structures analogous to the  $\eta^3$ -allyl complexes CpW(NO)( $\eta^3$ -C<sub>3</sub>H<sub>5</sub>)X (X = I,<sup>19b</sup> Cl<sup>19c</sup>), in which the allyl linkage is asymmetrically ( $\sigma$ ,  $\pi$ ) bound to the metal (*vide supra*).

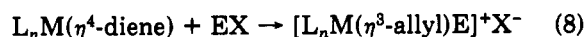
The IR spectra of 4–7 exhibit strong nitrosyl absorptions in the region expected for these types of complexes (i.e. 1650–1670 cm<sup>-1</sup>). These nitrosyl-stretching frequencies are 60–70 cm<sup>-1</sup> higher in energy than those of their respective diene-containing starting materials. This indicates that the metal center in these species is less electron rich than that in the  $\eta^4$ -diene complexes.

The <sup>1</sup>H NMR spectra of 4–7 (Table III) are very complex, as expected.<sup>19b,c</sup> Interestingly, the counterions in 4–7 change the chemical shifts of the signals in the <sup>1</sup>H NMR spectra, but no systematic pattern can be identified. The spectra of 5–7 show evidence for the existence of at least two isomers in solution. There is a possibility of four isomers in solution, i.e. the endo and exo isomers with the uncoordinated fragment of the allyl ligand on the same side as the X ligand or on the same side as the nitrosyl ligand, e.g. for 4–6



Furthermore, Faller<sup>19c</sup> has shown that in some of these systems the allyl complexes are fluxional in solution and interconvert when heated. Assignment of the <sup>1</sup>H NMR spectra of 4–7 during this work was therefore limited to the designation of a resonance to a proton on the carbon chain with no attempt being made to assign the isomers.

These  $\eta^3$ -allyl complexes are the expected products from the reaction of a diene complex with the reagent EX (E = electrophile; X = coordinating anion). The products resulting from the treatment of organometallic diene complexes [L<sub>n</sub>M( $\eta^4$ -diene)] with EX, where X is a noncoordinating anion, are expected to be the  $\eta^3$ -allyl cationic complexes, i.e.



(21) (a) Yasuda, H.; Kajihara, K.; Nagasuna, K.; Mashima, K.; Nakamura, A. *Chem. Lett.* 1981, 719. (b) Erker, G.; Engel, K.; Dorf, U.; Atwood, J.; Hunter, W. E. *Angew. Chem., Int. Ed. Engl.* 1982, 21, 914.

(22) (a) Kai, Y.; Kanehisa, N.; Miki, K.; Kasai, N.; Mashima, K.; Nagasuna, K.; Yasuda, H.; Nakamura, A. *Chem. Lett.* 1982, 1979. (b) Skibbe, V.; Erker, G. *J. Organomet. Chem.* 1983, 241, 15.

In fact, Wink and co-workers<sup>23</sup> have shown that in other systems this is a useful method for directing regio- and stereospecific electrophilic attack on a diene ligand.

Our attempts to isolate the products resulting from the reaction between a molybdenum *trans*-diene complex and HBF<sub>4</sub> have been unsuccessful and very frustrating. There appears to be more than one organometallic product of the reaction, as evidenced by a very broad (100 cm<sup>-1</sup>)  $\nu_{\text{NO}}$  band in the IR spectrum of the reaction mixture and several resonances in the Cp region of the proton NMR spectrum of the reaction residue. Furthermore, all attempts to separate and purify the mixture lead to decomposition of all nitrosyl-containing species. An interesting addendum to these observations is that, whatever the organometallic species are in the final reaction mixture, they are stable with respect to attack by H<sup>-</sup> (e.g. NaBH<sub>4</sub> and Red-Al).

In summary, it appears that more study of this latter area is needed in order to define properly the limits of the

reactions of the *trans*-diene complexes with electrophiles. For instance, our observations to date do not rule out that oxidation of the organometallic reactants may well also be occurring upon their treatment with H<sup>+</sup>. Nevertheless, it is also clear from the studies described in this paper that nucleophilic attack on the *trans*-diene complexes does not lead to concomitant reduction. Hence, these reactivity patterns are fully in accord with the molecular orbital description of the bonding of these interesting organometallic complexes.<sup>5</sup>

**Acknowledgment.** We are grateful to the Natural Sciences and Engineering Research Council of Canada for support of this work in the form of grants to P.L. and F.W.B.E.

**Supplementary Material Available:** Tables of positional and thermal parameters for the hydrogen atoms and anisotropic thermal parameters for the non-hydrogen atoms for each of the complexes 1A and 2 and bond lengths and bond angles involving the hydrogen atoms of 2 (10 pages); listings of the observed and calculated structure factors for both complexes (36 pages). Ordering information is given on any current masthead page.

(23) Wink, D. J.; Wang, N. F.; Springer, J. P. *Organometallics* 1989, 8, 259.

## Oxymethylation of Alkyliron Complex CpFe(CO)<sub>2</sub>-R with Hydrostannane and -silane, Leading to R-CH<sub>2</sub>OH Derivatives: Related Reactions of CpFe(CO)(L)-R and CpFe(CO)(L)-C(O)R Type Organoiron Complexes and the Molecular Structure of *trans*-CpFe(H)(CO)(SnPh<sub>3</sub>)<sub>2</sub>

Munetaka Akita,\* Tomoharu Oku, Masako Tanaka, and Yoshihiko Moro-oka\*

*Research Laboratory of Resources Utilization, Tokyo Institute of Technology, 4259 Nagatsuta, Midori-ku, Yokohama 227, Japan*

Received February 8, 1991

Thermal reaction of an alkyliron complex CpFe(CO)<sub>2</sub>-R (1) (R = CH<sub>2</sub>CH<sub>2</sub>Ph) and acyliron complexes, CpFe(CO)<sub>2</sub>-C(O)R (3) and CpFe(CO)(PPh<sub>3</sub>)-C(O)R (4) with 3 equiv of HMMe<sub>3</sub> (M = Sn, Si) affords the oxymethylated product R-CH<sub>2</sub>OX (5) in excellent yields accompanied by the formation of CpFe(H)(L)(MMe<sub>3</sub>)<sub>2</sub> (9a L = CO, M = Sn; 10a L = CO, M = Si; 11 L = PPh<sub>3</sub>, M = Sn). The reaction of a phosphine-substituted alkyliron complex CpFe(CO)(PPh<sub>3</sub>)-R (2) under similar reaction conditions gives R-H (7). On the other hand, irradiation of the organoiron complexes 1-4 in the presence of HMMe<sub>3</sub> produces 7 as a major product with the exception of 3 + HSnMe<sub>3</sub> where R-CHO (6) is obtained. The thermal reaction is found to consist of two consecutive reactions, i.e., formation of 6 and reduction of 6 to 5. When HSnMe<sub>3</sub> is used as a limiting substrate (HSnMe<sub>3</sub>/1 ≤ 2), R-CHO is actually formed in good yield. The second step is proved to be catalyzed by various iron complexes such as 9a, Fp-Me, Fp-C(O)Me, and Fp<sub>2</sub>. The relationship among 1-4 and the coordinatively unsaturated species is also discussed. The molecular structure of *trans*-CpFe(H)(CO)SnPh<sub>3</sub>)<sub>2</sub> (9c) obtained by the thermal reaction of 1 with HSnPh<sub>3</sub> has been determined by X-ray diffraction study. The unit cell contains two crystallography independent molecules with the essentially same geometry. The structure is described as a four-legged piano stool structure with the two SnPh<sub>3</sub> groups occupying the mutually *trans* basal positions. The contribution of the  $\eta^2$ -coordination mode of the H-Sn bond may be negligible on the basis of the molecular structure as well as the small <sup>2</sup>J(H-Fe-Sn) values. Crystal data for 9c: space group *P* $\bar{1}$ , *a* = 16.248 (7) Å, *b* = 19.646 (6) Å, *c* = 11.443 (5) Å,  $\alpha$  = 93.32 (3)°,  $\beta$  = 93.67 (4)°,  $\gamma$  = 97.09 (3)°, *V* = 3609 (3) Å<sup>3</sup>, *Z* = 4, *R* = 0.0312, *R*<sub>w</sub> = 0.0379.

### Introduction

Reductive cleavage of a transition metal-carbon bond plays an important role in the product-releasing step of a variety of catalytic reactions including hydrogenation and hydroformylation.<sup>1</sup> For example, in the former reaction oxidative addition of hydrogen to an alkylmetal species leads to the formation of a (dihydrido)(alkyl)metal species, which reductively eliminates the product, alkane.

On the other hand, it has been revealed that hydrosilane and -stannane exhibit reactivities similar to those of hydrogen with respect to oxidative addition to a low-valent metal center.<sup>1,2</sup> In addition to this feature, silicon and tin

(1) Collman, J. P.; Hegedus, L. S.; Norton, J. R.; Finke, R. G. *Principles and Applications of Organotransition Metal Chemistry*, 2nd ed.; University Science Book: Mill Valley, CA, 1987.